



SIMULATION OPTIMIZATION SYSTEMS
Research Laboratory

**ELECTROMAGNETIC DESIGN
OF HIGH-TEMPERATURE
SUPERCONDUCTING MICROWAVE FILTERS**

**J.W. Bandler, R.M. Biernacki, S.H. Chen,
W.J. Getsinger, P.A. Grobelny,
C. Moskowitz and S.H. Talisa**

SOS-95-1-R

January 1995

(Revised April 1995)



**ELECTROMAGNETIC DESIGN
OF HIGH-TEMPERATURE
SUPERCONDUCTING MICROWAVE FILTERS**

**J.W. Bandler, R.M. Biernacki, S.H. Chen,
W.J. Getsinger, P.A. Grobelny,
C. Moskowitz and S.H. Talisa**

SOS-95-1-R

January 1995

(Revised April 1995)

**© J.W. Bandler, R.M. Biernacki, S.H. Chen, W.J. Getsinger,
P.A. Grobelny, C. Moskowitz and S.H. Talisa 1995**

No part of this document may be copied, translated, transcribed or entered in any form into any machine without written permission. Address enquiries in this regard to Dr. J.W. Bandler. Excerpts may be quoted for scholarly purposes with full acknowledgement of source. This document may not be lent or circulated without this title page and its original cover.

**ELECTROMAGNETIC DESIGN
OF HIGH-TEMPERATURE SUPERCONDUCTING MICROWAVE FILTERS**

J.W. Bandler,^{*} R.M. Biernacki,^{*} S.H. Chen,^{*}
W.J. Getsinger,^{**} P.A. Grobelny,^{*}
C. Moskowitz^{***} and S.H. Talisa^{****}

Abstract

We present novel approaches to electromagnetic design of high-temperature superconducting (HTS) quarter-wave parallel coupled-line microstrip filters. The desired narrow bandwidths (less than 2%) coupled with the large dielectric constant of substrate materials used in the HTS technology ($\epsilon_r \approx 24$) make the design problems difficult to be accurately treated by many traditional microwave circuit design software packages with analytical/empirical models. We have successfully performed an HTS filter design with accurate electromagnetic field simulations. We discuss problems related to electromagnetic design of such filters. We describe a look-up table method and a powerful space mapping optimization technique, which dramatically reduce the CPU time needed in the design process. Finally, we address the issue of improved modeling of the HTS filter using analytical/empirical models.

This work was supported in part by Optimization Systems Associates Inc.; in part by the Natural Sciences and Engineering Research Council of Canada under Grants OGP0007239, OGP0042444 and STR0117819; and in part by the U.S. Navy under contracts N00014-92-C-2043 and N00014-91-C-0112.

^{*} J.W. Bandler, R.M. Biernacki and S.H. Chen are with Optimization Systems Associates Inc. They are also with and P.A. Grobelny is with the Simulation Optimization Systems Research Laboratory and Department of Electrical and Computer Engineering, McMaster University, Hamilton, Ontario, Canada L8S 4L7.

^{**} W.J. Getsinger, 6662 Bozman-Neavitt Rd., Bozman, MD 21612.

^{***} C. Moskowitz was with the Westinghouse Electronic Systems Group, Baltimore, MD 21203.

^{****} S.H. Talisa is with the Westinghouse Science and Technology Center, Pittsburgh, PA 15235.

I. INTRODUCTION

The recently discovered high-temperature superconductors (HTS) are of great potential for passive microwave military and commercial applications. Available low-loss and narrow-bandwidth (0.5 - 3%) filter banks are of very large size, which in some satellite and airborne applications is intolerable. Small conventional microstrip filters are too lossy for narrow-band applications. Using HTS technology [1, 2], however, low-loss, narrow-bandwidth microstrip filters, requiring relatively inexpensive cooling, can be made.

Advances in electromagnetic (EM) simulation provide designers with the opportunity to accurately simulate passive microstrip circuits. We verified the usefulness of EM simulation in analyzing circuits built with the HTS technology by simulating two existing HTS microstrip filters which had been designed using conventional techniques. In both cases good correlation was observed between the EM simulated and measured responses.

In this paper we concentrate on the design of an HTS quarter-wave parallel coupled-line filter using an EM simulator. The difficulty arising here is related to the large dielectric constant of the substrate materials ($\epsilon_r \approx 24$) used in the HTS technology and the inability of the traditional analytical/empirical models to accurately analyze structures built of such materials. To overcome this problem we resort to EM field simulations which can provide results that are in good agreement with experimental data. This, however, is at the expense of a very high computational cost, particularly in simulating narrow-bandwidth filters whose inherent high sensitivity to dimensional changes calls for a very fine grid in the numerical EM simulation.

In order to decrease the CPU time required for the overall design process and to overcome the high sensitivity of the filter, in fact to successfully complete the design, we considered two approaches. The first approach is based on a table of coupling versus gap and frequency values and the second is based on a novel space mapping (SM) circuit optimization [3-5]. In the look-up table approach we analyze the couplings in different sections of the filter for different gaps in each of the sections swept over the frequency band of interest. The couplings are determined from EM simulations and the table is iteratively updated. In the SM approach an adaptive mapping between

an OSA90/hope [6] simulation model and *em* [7, 8] simulations is established. Such a mapping allows us to benefit from the accuracy of EM simulations while using a much faster model for optimization. The SM method is a novel extension of our work on optimization-driven EM simulation [9, 10]. The method was tested using OSA90/hope interfaced to *em* through Empipe [6].

In Section II we describe the filter to be designed. In Section III we show the inability of the traditional simulators with analytical/empirical models to accurately model the HTS filter. Section IV includes examples demonstrating the usefulness of EM simulators in analyzing HTS filters. In this section we also discuss some issues specific to EM simulation of the HTS filters. In Section V we describe problems arising when geometrical interpolation is applied to EM simulations of narrow-bandwidth HTS filters. The look-up table method and the SM optimization technique as applied to the design of the HTS filter are described in Sections VI and VII, respectively. Section VIII contains a discussion on improving the analytical/empirical model of the filter. Finally, Section IX contains our conclusions.

II. THE FILTER

We wish to design a four-pole quarter-wave parallel coupled-line microstrip filter. The geometry of the filter is shown in Fig. 1. L_1 , L_2 and L_3 are the lengths of the parallel coupled-line sections and S_1 , S_2 and S_3 are the gaps between the sections. The width W is the same for all the sections as well as for the input and output microstrip lines, of length L_0 . The thickness of the lanthanum aluminate substrate used is 20 mil. The dielectric constant and the loss tangent are assumed to be 23.425 and 3×10^{-5} , respectively. The metallization is considered lossless. The design specifications are as follows.

$$|S_{21}| \leq 0.05 \quad \text{for} \quad f \leq 3.967 \text{ GHz and } f \geq 4.099 \text{ GHz}$$

$$|S_{21}| \geq 0.95 \quad \text{for} \quad 4.008 \text{ GHz} \leq f \leq 4.058 \text{ GHz}$$

This corresponds to a 1.25% bandwidth. L_1 , L_2 , L_3 , S_1 , S_2 and S_3 are the design parameters. L_0 and W are fixed.

We approach the filter design by employing both the traditional analytical/empirical models and EM simulations.

III. FILTER DESIGN USING TRADITIONAL SIMULATORS

Computer aided filter design involves minimization of a scalar objective function U which is a measure of the deviation of the filter responses from the imposed design specifications. In order to formulate U we consider error functions defined as

$$e_j(\mathbf{x}) = R_j(\mathbf{x}) - S_{uj} \quad \text{or} \quad e_j(\mathbf{x}) = S_{lj} - R_j(\mathbf{x}) \quad (1)$$

where S_{uj} and S_{lj} are the upper and lower specifications, respectively, and $R_j(\mathbf{x})$ is the response of the filter at a given point of designable variables \mathbf{x} . Errors $e_j(\mathbf{x})$ are computed at frequencies for which S_{uj} and/or S_{lj} are specified. A negative error value indicates that the corresponding specification is satisfied. For positive error values the corresponding specifications are violated.

The objective function U may be the generalized ℓ_p function [11] defined as

$$U = \begin{cases} \left[\sum_{\mathbf{i} \in \mathbf{J}} e_{\mathbf{i}}(\mathbf{x})^p \right]^{1/p} & \text{if } \mathbf{x} \notin A \\ - \left[\sum_{\mathbf{i}=1}^{\mathbf{M}} (-e_{\mathbf{i}}(\mathbf{x}))^p \right]^{1/p} & \text{if } \mathbf{x} \in A \end{cases} \quad (2)$$

where the index set \mathbf{J} is given as

$$\mathbf{J} = \{ j \mid e_{\mathbf{j}}(\mathbf{x}) \geq 0 \} \quad (3)$$

and the acceptability region A is defined as

$$A = \{ \mathbf{x} \mid e_{\mathbf{j}}(\mathbf{x}) < 0 \quad j = 1, 2, \dots, M \} \quad (4)$$

M is the total number of error functions. By letting $p = \infty$ we have the minimax objective

$$U = \max_{\mathbf{i}} \{ e_{\mathbf{i}}(\mathbf{x}) \} \quad (5)$$

which is used in our design of the HTS filter.

We started the design of our HTS filter by optimizing the filter using two commercial microwave CAD packages, namely, OSA90/hope [6] and Touchstone [12]. The minimax solutions are listed in the first two columns of Table I. Subsequently, we performed *em* simulations at both solutions. The *em* simulation results differed from the circuit simulation results and did not satisfy

the specifications. The $|S_{21}|$ and $|S_{11}|$ responses are shown in Figs. 2 and 3. Although the corresponding filters were not built and, therefore, measurements were not available, EM simulations indicate that inaccurate models in traditional simulators may lead to inadequate designs of HTS filters. Nevertheless, such models can still be used as a tool to obtain a starting point for further EM based design.

IV. EM SIMULATION OF HTS FILTERS

To investigate the usefulness of EM simulation in analyzing circuits built in the HTS technology we simulated and measured two existing HTS microstrip filters. The filters together with the corresponding measurements and EM simulation results are shown in Figs. 4 and 5. In both cases good correlation can be observed between the measured and simulated responses. The shapes of the responses are nearly identical. The frequency shift between the measured and simulated responses is most likely due to the discrete nature of the numerical EM analysis introducing rounding of the geometrical dimensions of the filters to the EM simulation grid (see Section V) and/or to using a simulation grid which was not fine enough. Among other factors that may also contribute to discrepancies between EM simulations and measurements are possible measurement errors and calibration problems, non-uniformity of the dielectric constant and height of the substrate material, inaccuracy in simulating losses, etc.

The simulation grid, or simply grid, is defined by the user and is imposed on the analyzed structure during numerical EM analysis. In general, using a finer grid (larger number of grid points) makes the analysis time longer and the analysis results more accurate. Using a coarser grid (smaller number of grid points) shortens the analysis time but may degenerate the accuracy of the results. Therefore, it is very important to select a grid that would make EM analysis not only as efficient as possible but also sufficiently accurate.

For the HTS quarter-wave parallel coupled-line microstrip filter the accuracy of the results depends heavily on the grid size used in the EM analysis. To define the uniform grid used by the *em* [7] simulator we need to select two grid spacings Δx and Δy .

Fig. 6 shows the EM simulated responses of $|S_{21}|$ of the filter in an early stage of the design process obtained using different grids. In particular, we fixed the grid spacing in the x direction at $\Delta x = 5$ mil and used three different grid spacings in the y direction: $\Delta y_1 = 3.5$ mil, $\Delta y_2 = 1.75$ mil and $\Delta y_3 = 0.875$ mil. For all three grids the geometry of the circuit was kept unchanged with the following values of the geometrical parameters: $L_0 = 50$ mil, $W = 7$ mil, $L_1 = L_2 = L_3 = 190$ mil, $S_1 = 21$ mil, $S_2 = 94.5$ mil and $S_3 = 108.5$ mil. It can be seen from Fig. 6 that using different grid sizes preserved the shape of the response but resulted in a shift of the center frequency of the filter. Moreover, comparing the responses obtained using grid spacings Δy_1 and Δy_2 and then Δy_2 and Δy_3 shows that the difference in the shift becomes smaller for smaller grid spacings. It is worth pointing out that in all cases considered the number of cells per wavelength well exceeded the recommended minimum of 20.

This phenomenon forces the use of a finer grid for EM simulations in order to preserve the accuracy of the results. This becomes even more significant if very small bandwidths are desired which makes the circuit responses very sensitive to dimensional changes. For other applications a 10 MHz shift in the center frequency, as observed in Fig. 6, could be negligibly small but for the considered HTS filter it corresponds to 20% of the bandwidth. In our analysis we set the grid spacings to $\Delta x = 1$ mil and $\Delta y = 1.75$ mil. Therefore, the overall grid for *em* simulations was approximately 1000×250. Subsectioning is not directly controlled by the user, but the limits of a maximum of 100 cells per subsection and a minimum of 20 subsections per wavelength were used. This resulted in about one CPU hour needed to simulate the filter at a single frequency on a Sun SPARCstation 10.

V. ELECTROMAGNETIC DESIGN WITH GEOMETRICAL INTERPOLATION

One of the main characteristics of *em*, which employs a uniform grid, is discretization of geometrical dimensions. If a parameter is off the grid the simulator will automatically snap it to the closest on-grid value. Thus, analysis can only be performed for discrete or on-grid values of the parameters defining the geometry of the circuit. Whenever a response for an off-grid point is required we employ geometrical interpolation to estimate the response. Utilizing geometrical

interpolation makes it possible to provide a gradient based optimizer with continuous responses and smooth gradients of the responses [9, 10].

Geometrical interpolation applied to typical microwave circuits proved to be efficient and accurate [9, 10]. However, it failed for this particular HTS filter. Fig. 7 explains why. It shows three $|S_{21}|$ responses of the filter obtained at three different points, i.e., sets of the geometrical parameters. The grid spacings used are $\Delta x = 2.5$ mil and $\Delta y = 1.75$ mil. Two of the points are on the grid and the third one is an off-grid point. Geometrical interpolation is used to determine the S parameters at the third, off-grid point by interpolating the values of the S parameters calculated by *em* at the first two points (the real and imaginary parts are interpolated independently). All three lengths L_1 , L_2 and L_3 are set to 190 mil and 192.5 mil for the first and the second point, respectively, clearly on the grid. For the third point $L_1 = L_2 = L_3 = 191.25$ mil (clearly, off the grid). All other parameters have the same values at all three points: L_0 , W , S_1 , S_2 , S_3 are set to 50, 7, 21, 94.5 and 108.5 mil, respectively. As shown in Fig. 7, and similar to Fig. 6, the frequency responses at the first two points exhibit a significant shift of the center frequency which is due to the change in parameter values as small as one grid spacing. This shift makes geometrical interpolation inaccurate. For the interpolated response at the third point one would expect a similar shape of the response. That response should be shifted approximately half way between the responses at the first two points. However, the actually interpolated response for the third, off-grid, point does not resemble the other two: it has a much wider passband with a deep notch in the passband. In principle, the accuracy of the interpolation could be improved by using much finer grid spacings but this would make the EM simulation time prohibitively long.

Our methods allow us to select on-grid parameter values for *em* simulations, thus avoiding the potential pitfalls associated with geometrical interpolation.

VI. FILTER DESIGN USING THE LOOK-UP TABLE METHOD

Although the technique is general in nature, it has been applied only to the class of filters known as parallel coupled-line filters which are derivable from lowpass ladder networks. One starts with the normalized lowpass ladder network elements which satisfy some predetermined shape

requirement and results in the lowpass prototype element values also known as the g values. An appropriate bandpass and impedance transformation is performed which leads to good approximations of the even and odd mode impedances of the coupled-line sections which comprise the filter. The next step in the design process is to determine the geometry or conductor arrangement which realizes this set of even/odd mode impedances. The medium that we have chosen is microstrip on 20 mil lanthanum aluminate. In this medium, the coupled sections are characterized by three geometric parameters; line width, coupling length and coupling gap, which must be chosen to provide the required even and odd mode impedances. The ratio of these impedances depends only on the coupling coefficient of the coupler and the product depends on the impedance level.

The simulator aided design process consists of estimating the quarter wavelength in the medium at filter band center, and the gap required for the coupling. One then constructs a geometry for the EM simulator which consists of a coupled-line with input and output ports on a diagonal with the other diagonal remaining as open circuits. Actually, several geometries are constructed over a range of gaps so that one can interpolate the *em* simulator's results to the required gap based upon the required coupling factor. This process is repeated for each coupled section of the filter. When a complete set of gaps has been determined by interpolation, the filter is analyzed by the EM simulator. The result usually has a shape that is close to the desired shape but is offset in center frequency. The amount of the frequency error and the original coupling length provide enough information to compute a length correction, i.e., the fractional change in frequency is proportional to the negative of the fractional change in length. The process is then repeated using the new coupling length.

The filter's $|S_{21}|$ and $|S_{11}|$ responses simulated by *em* at the look-up table method solution are shown in Figs. 8 and 9, respectively. The solution point is listed in the third column of Table I. The $|S_{21}|$ response has the desired shape but the center frequency is slightly shifted w.r.t. specifications. Also, a small ripple present in the passband, see Fig. 8(b), results in non-uniform $|S_{11}|$ in the passband.

VII. FILTER DESIGN USING THE SPACE-MAPPING METHOD

In its basic form, the SM optimization technique [5] exploits a mathematical link between input parameters of two simulators (models). One is considered very accurate but computationally very intensive while the other one is fast but less accurate. The goal is to direct the bulk of CPU intensive optimization to the fast model in the optimization system (OS) parameter space X_{OS} . This model is referred to as the OS simulator. EM simulations serve as the accurate model and the EM simulator input parameter space is denoted by X_{EM} . As a first step in SM optimization we carry out conventional design optimization entirely in the X_{OS} space. The resulting solution is denoted by \mathbf{x}_{OS}^* . Then, we create and iteratively refine a mapping

$$\mathbf{x}_{OS} = P(\mathbf{x}_{EM}) \quad (6)$$

from X_{EM} to X_{OS} in order to align the two models.

In principle, the choice of the mathematical form of the mapping is an implementational issue. In [5] we only assume that the mapping can be expressed as a linear combination of some predefined and fixed fundamental functions. In the current implementation of SM we also assume that P is invertible. Once the mapping is established the inverse mapping P^{-1} is used to find the EM solution as the image of the optimal OS solution \mathbf{x}_{OS}^* , namely,

$$\bar{\mathbf{x}}_{EM} = P^{-1}(\mathbf{x}_{OS}^*) \quad (7)$$

In other words, we map the optimal OS model parameters back into the EM parameters (e.g., physical layout).

P is established through an iterative process. The initial mapping $P^{(0)}$ is found using a preselected set B_{EM} of k points in X_{EM} and the set B_{OS} of corresponding points in X_{OS} . The number k of these base points should be sufficient to uniquely determine all the coefficients at the fundamental functions defining the mapping. Their selection is fairly arbitrary although, for the reasons discussed in Section V, we select these points on the grid. The points in B_{OS} are determined by k auxiliary optimizations to achieve

$$f_{OS}(\mathbf{x}_{OS}^i) \approx f_{EM}(\mathbf{x}_{EM}^i), \quad i = 1, 2, \dots, k \quad (8)$$

where f_{OS} and f_{EM} are the circuit responses simulated by the OS and EM simulators, respectively. This may be referred to as a parameter extraction (fit). In other words, we optimize the OS model to fit its response to the EM simulator response calculated at x_{EM}^i . In this optimization the OS model parameters x_{OS} are the optimization variables. As a result we find the point x_{OS}^i . This process is repeated for all the base points.

At the j th iteration B_{EM} is expanded by the new image of x_{OS}^* computed using $(P^j)^{-1}$ and snapped to the grid. B_{OS} is expanded accordingly. The iterations continue until

$$\|f_{EM}(\bar{x}_{EM}) - f_{OS}(x_{OS}^*)\| \leq \epsilon \quad (9)$$

where $\|\cdot\|$ indicates a suitable norm and ϵ is a small positive constant. In the process of finding the mapping an overdetermined system of equations may need to be solved. In such situations, optimization techniques, such as least-squares, can be used.

Applying the SM optimization technique to the design of the HTS filter we used the Empire interface interconnecting *em* to OSA90/hope [6]. All the processing needed to establish the mapping was performed within the OSA90/hope environment.

A total of 13 *em* simulations was sufficient to establish the mapping P which satisfies (9) for this filter. To satisfy the match implied by (8) we used the ℓ_1 optimizer. For a matching problem the ℓ_1 objective is defined by

$$U = \sum_{i=1}^M |e_i| \quad (10)$$

where M is the number of error functions, which are derived directly from (8). The properties of the ℓ_1 objective are superior in data fitting, parameter extraction and other applications involving matching of responses. The point \bar{x}_{EM} obtained as the $(P)^{-1}$ image of x_{OS}^* is listed in the fourth column of Table I. It gave us an excellent response of the filter, as simulated by *em*. The $|S_{21}|$ response, shown in Fig. 10, meets the design specifications well. The $|S_{11}|$ response, shown in Fig. 11, is also improved.

VIII. IMPROVING THE ANALYTICAL/EMPIRICAL MODEL OF THE FILTER

It is desirable to create a fast and accurate model of the HTS filter for the optimal set of the parameter values. Such a model can be used for efficient analysis of the filter especially in situations where the filter is a subcircuit of a larger circuit.

Fig. 12 compares the optimal $|S_{21}|$ response of the filter obtained using OSA90/hope [6] analytical/empirical microstrip models with the EM simulated SM solution. OSA90/hope's result corresponds to \mathbf{x}_{OS}^* - the optimal point in the OS space, and the EM response corresponds to $\bar{\mathbf{x}}_{EM}$ obtained using (7) that is to the true physical dimensions. Good agreement can be observed in the passband region but the responses become significantly different for the stopband frequencies. In particular, there is a notch in the EM simulated response which is completely missing in the analytical/empirical model response. Similar notch or notches are observed in measurements of other microstrip filters (see Figs. 4 and 5). The presence of the notch(es) in the filter response is undesirable.

We expanded the analytical/empirical model by adding a lumped inductor directly between the input and the output of the filter. Subsequently, we optimized the value of this inductance so that the responses of the analytical/empirical model of the filter best match the EM simulated responses of the filter. We used the ℓ_1 optimizer for optimization. The optimal value of the inductor is $L = 0.43 \mu\text{H}$. The match between the responses of the analytical/empirical model with the inductor and the EM model is very good. It is shown in Fig. 13. To model the phenomena related to the ground currents by a single lumped inductor is a simplified approach. Nonetheless, the resulting model of the filter is quite accurate. What is important in this experiment is that frequently a simple modification to the analytical/empirical model will result in improved match of its responses to the EM simulator responses. Such models could significantly ease the parameter extraction phase of the SM process.

IX. CONCLUSIONS

We have demonstrated the difficulties of the traditional analytical/empirical models to accurately model narrow-band quarter-wave parallel coupled-line microstrip filters built using the HTS technology. We have discussed problems associated with utilizing EM simulations in design of such filters. In particular, we have briefly addressed the influence of the size of the EM grid and the discretization of geometrical parameters present in some numerical EM simulators. We have shown how geometrical interpolation, introduced to overcome the discretization problem, may fail due to the high sensitivity of the filter responses to dimensional changes, particularly for narrow-band HTS filters. Subsequently, we have applied two methods for EM-based design optimization of a parallel coupled-line microstrip filter to be built using the HTS technology. Excellent results have been obtained using the recent space mapping optimization technique [3, 5] which is a general approach that can be applied to other design problems. It is especially attractive for designs involving CPU intensive simulators, where it substantially decreases the number of necessary simulations and redirects the bulk of CPU intensive optimization to the fast model in the optimization system parameter space. The very recent development of "aggressive space mapping" [13] leads to even more reduction of EM simulation effort. This is achieved by best targeting every valuable EM simulation. We have also presented a simple modification to the analytical/empirical model that can improve the predictive capability of the fast model.

ACKNOWLEDGEMENT

The authors wish to thank Dr. J.C. Rautio of Sonnet Software, Inc., Liverpool, NY, for making *em* available for this work. The substantial comments of the reviewers are also greatly appreciated.

REFERENCES

1. S.H. Talisa, M.A. Janocko, C. Moskowitz, J. Talvacchio, J.F. Billing, R. Brown, D.C. Buck, C.K. Jones, B.R. McAvoy, G.R. Wagner and D.H. Watt, "Low- and high-temperature superconducting microwave filters," *IEEE Trans. Microwave Theory Tech.*, vol. 39, 1991, pp. 1448-1454.
2. W.G. Lyons, R.R. Bonetti, A.E. Williams, P.M. Mankiewich, M.L. O'Malley, J.M. Hamm, A.C. Anderson, R.S. Withers, A. Meulenberg and R.E. Howard, "High- T_c superconductive microwave filters," *IEEE Trans. Magnetics*, vol. 27, 1991, pp. 2537-2539.
3. J.W. Bandler, R.M. Biernacki, S.H. Chen, P.A. Grobelny, C. Moskowitz and S.H. Talisa, "Electromagnetic design of high-temperature superconducting microwave filters," *IEEE MTT-S Int. Microwave Symp. Digest* (San Diego, CA), 1994, pp. 993-996.
4. J.W. Bandler, R.M. Biernacki, S.H. Chen, P.A. Grobelny and R.H. Hemmers, "Exploitation of coarse grid for electromagnetic optimization," *IEEE MTT-S Int. Microwave Symp. Digest* (San Diego, CA), 1994, pp. 381-384.
5. J.W. Bandler, R.M. Biernacki, S.H. Chen, P.A. Grobelny and R.H. Hemmers, "Space mapping technique for electromagnetic optimization," *IEEE Trans. Microwave Theory Tech.*, vol. 42, 1994, pp. 2536-2544.
6. *OSA90/hope™* and *Empipe™*, Optimization Systems Associates Inc., P.O. Box 8083, Dundas, Ontario, Canada L9H 5E7, 1994.
7. *Em User's Manual* and *Xgeom User's Manual*, Sonnet Software, Inc., 135 Old Cove Road, Suite 203, Liverpool, NY 13090-3774, 1994.
8. J.C. Rautio and R.F. Harrington, "An electromagnetic time-harmonic analysis of arbitrary microstrip circuits," *IEEE Trans. Microwave Theory Tech.*, vol. 35, 1987, pp. 726-730.
9. J.W. Bandler, S. Ye, R.M. Biernacki, S.H. Chen and D.G. Swanson, Jr., "Minimax microstrip filter design using direct EM field simulation," *IEEE MTT-S Int. Microwave Symp. Digest* (Atlanta, GA), 1993, pp. 889-892.
10. J.W. Bandler, R.M. Biernacki, S.H. Chen, P.A. Grobelny and S. Ye, "Yield-driven electromagnetic optimization via multilevel multidimensional models," *IEEE Trans. Microwave Theory Tech.*, vol. 41, 1993, pp. 2269-2278.
11. J.W. Bandler and S.H. Chen, "Circuit optimization: the state of the art," *IEEE Trans. Microwave Theory Tech.*, vol. 36, 1988, pp. 424-443.
12. *Touchstone® Reference Manual Version 3.0*, EEsof, Inc., 5601 Lindero Canyon Road, Westlake Village, CA 91362-4020, 1991.
13. J.W. Bandler, R.M. Biernacki, S.H. Chen, R.H. Hemmers and K. Madsen, "Aggressive space for electromagnetic design," *IEEE MTT-S Int. Microwave Symp. Digest* (Orlando, FL), 1995, pp. xxx-xxx.

Figure Captions

- Fig. 1. The structure of the HTS quarter-wave parallel coupled-line microstrip filter (to scale). The dielectric constant and the substrate thickness are 23.425 and 20 mil, respectively. The geometrical dimensions are listed in Table I. The x and y grid sizes for *em* simulations are 1.0 and 1.75 mil. About 1 CPU hour is needed for analysis at a single frequency on a Sun SPARCstation 10.
- Fig. 2. The optimal solutions (solid lines) of (a) $|S_{21}|$ and (b) $|S_{11}|$ obtained using OSA90/hope. The corresponding *em* simulation results are shown as dashed lines. ∇ indicate upper and \wedge indicate lower specifications.
- Fig. 3. The optimal solutions (solid lines) of (a) $|S_{21}|$ and (b) $|S_{11}|$ obtained using Touchstone. The corresponding *em* simulation results are shown as dashed lines. ∇ indicate upper and \wedge indicate lower specifications.
- Fig. 4. Comparison between measured and EM simulated responses of the HTS filter shown in (a). (b) and (c) show measured and *em* simulated responses, respectively.
- Fig. 5. Comparison between measured and EM simulated responses of the HTS filter shown in (a). (b) and (c) show measured and *em* simulated responses, respectively.
- Fig. 6. The *em* simulated $|S_{21}|$ response of the HTS parallel coupled-line filter obtained in an early stage of the design process for different grid sizes. The grid size in the x direction is $\Delta x = 5$ mil and it is kept fixed. The grid sizes in the y direction are $\Delta y_1 = 3.5$ mil (solid line), $\Delta y_2 = 1.75$ mil (dashed line) and $\Delta y_3 = 0.875$ mil (dotted line).
- Fig. 7. Illustration of utilizing the geometrical interpolation in the design of the HTS parallel coupled-line microstrip filter. The $|S_{21}|$ responses for $L_1 = L_2 = L_3 = L = 190$ and 192.5 mil (solid lines) do not involve geometrical interpolation. The response for $L_1 = L_2 = L_3 = L = 191.25$ mil (dashed line) is interpolated and clearly incorrect. Circles indicate analyzed frequency points.
- Fig. 8. The *em* simulated $|S_{21}|$ response of the HTS parallel coupled-line filter at the solution obtained using the look-up table method. (a) Response for the overall band. (b) Passband details of the response. ∇ and \wedge indicate upper and lower specifications, respectively. The response exhibits the desired shape with slightly shifted center frequency.
- Fig. 9. The *em* simulated $|S_{11}|$ response of the HTS parallel coupled-line filter at the solution obtained using the look-up table method.
- Fig. 10. The *em* simulated $|S_{21}|$ response of the HTS parallel coupled-line filter at the solution obtained using the SM optimization method. (a) Response for the overall band. (b) Passband details of the response. ∇ and \wedge indicate upper and lower specifications, respectively.
- Fig. 11. The *em* simulated $|S_{11}|$ response of the HTS parallel coupled-line filter at the solution obtained using the SM optimization method.
- Fig. 12. Comparison between the optimal $|S_{21}|$ response of the HTS parallel coupled-line filter obtained using the analytical/empirical model (dashed line) and the EM simulated SM solution (solid line). (a) Response for the overall band. (b) Passband details of the response.
- Fig. 13. Modeling of the notch in the $|S_{21}|$ response of the HTS parallel coupled-line filter. In order to model the notch we introduced an inductor between the input and output of the filter. The analytical/empirical model response is shown as a dashed line. The EM simulated response is shown as a solid line. (a) Response of the overall band. (b) Passband details of the response.

Bandler *et al.* "Electromagnetic design of HTS filters", Table I

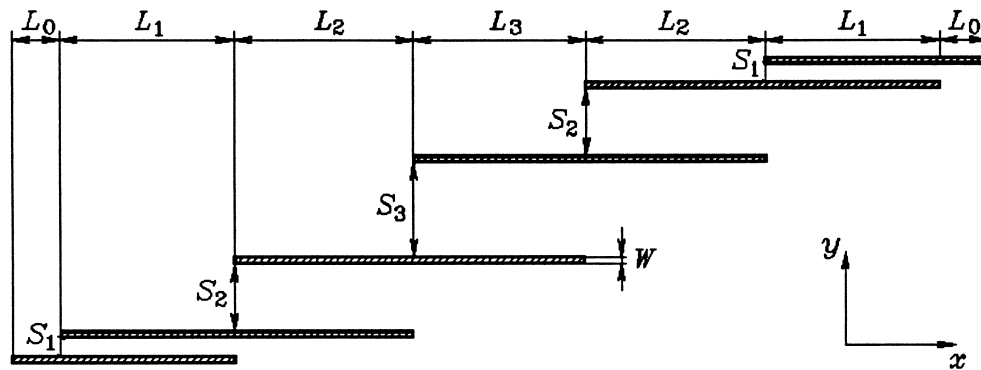
International Journal of Microwave and Millimeter-Wave Computer-Aided Engineering, vol. 5, 1995, Special Issue on Engineering Applications of Electromagnetic Field Solvers.

TABLE I
HTS PARALLEL COUPLED-LINE MICROSTRIP
FILTER DESIGN RESULTS

Parameter (mil)	OSA90/hope Optimization	Touchstone Optimization	Look-up Table Method	SM Method
L_1	191.00	188.70	188.70	190.00
S_1	21.74	22.52	20.88	19.25
L_2	195.58	188.11	188.10	192.00
S_2	96.00	93.19	76.02	75.25
L_3	191.00	188.58	188.59	189.00
S_3	114.68	109.13	85.07	91.00
W	7.00	6.93	6.93	7.00
L_0	50.00	50.00	50.00	50.00

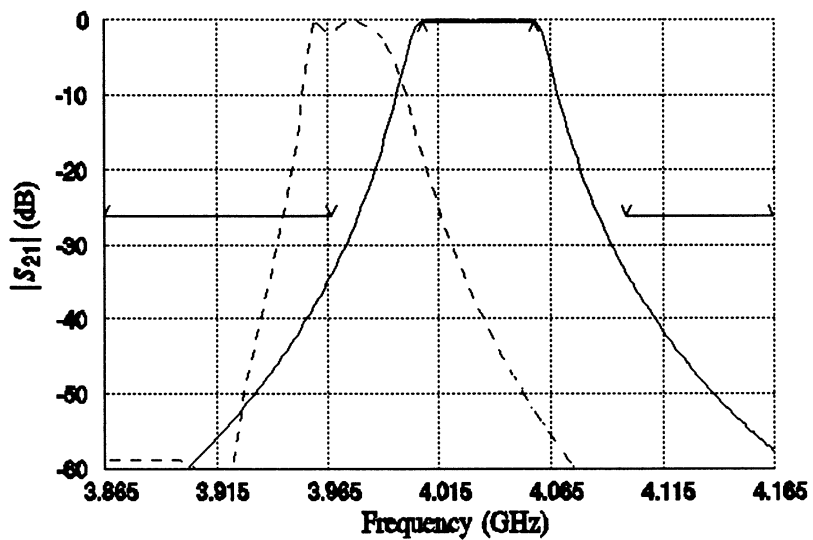
Bandler *et al.* "Electromagnetic design of HTS filters", **Figure 1**

International Journal of Microwave and Millimeter-Wave Computer-Aided Engineering, vol. 5, 1995,
Special Issue on Engineering Applications of Electromagnetic Field Solvers.

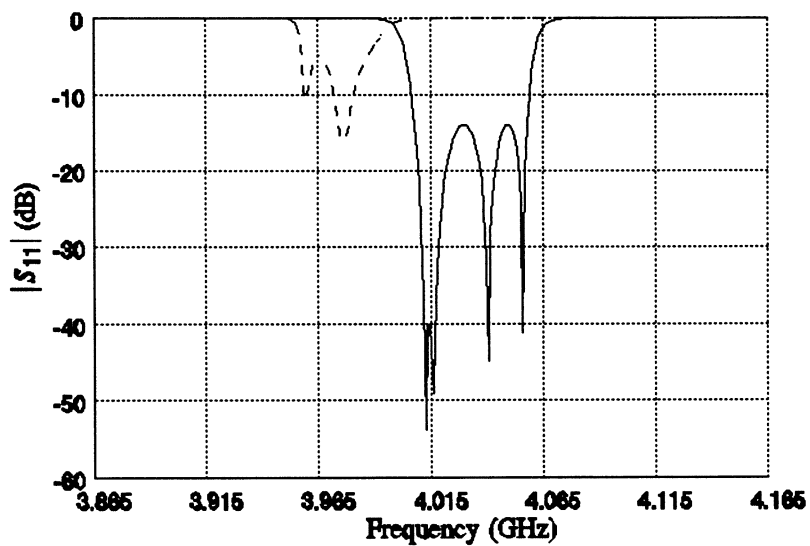


Bandler *et al.* "Electromagnetic design of HTS filters", **Figure 2**

International Journal of Microwave and Millimeter-Wave Computer-Aided Engineering, vol. 5, 1995, Special Issue on Engineering Applications of Electromagnetic Field Solvers.



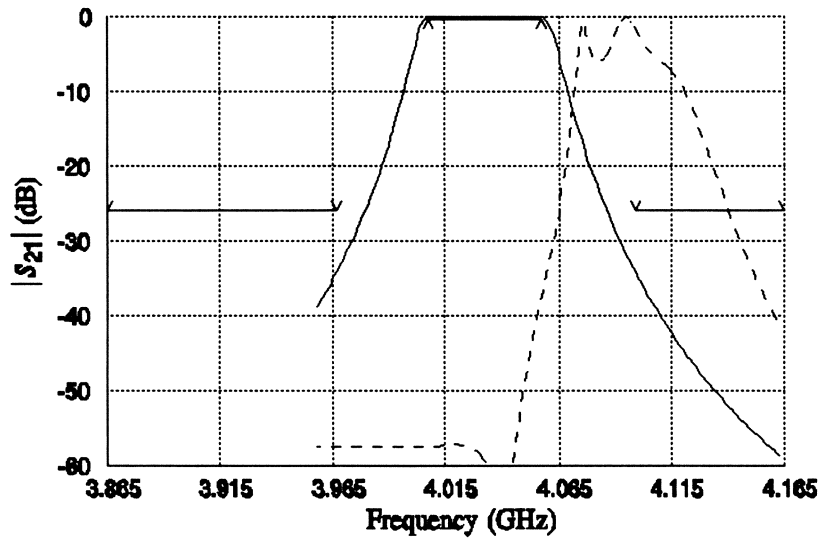
(a)



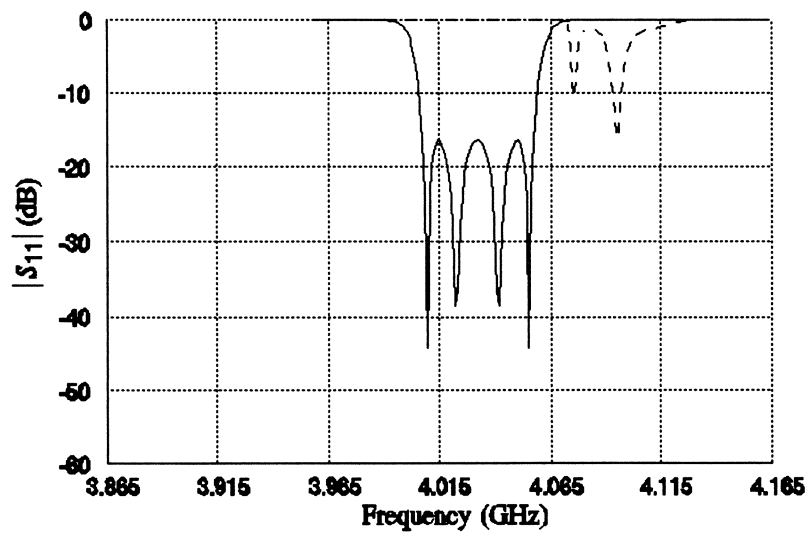
(b)

Bandler *et al.* "Electromagnetic design of HTS filters", **Figure 3**

International Journal of Microwave and Millimeter-Wave Computer-Aided Engineering, vol. 5, 1995, Special Issue on Engineering Applications of Electromagnetic Field Solvers.



(a)



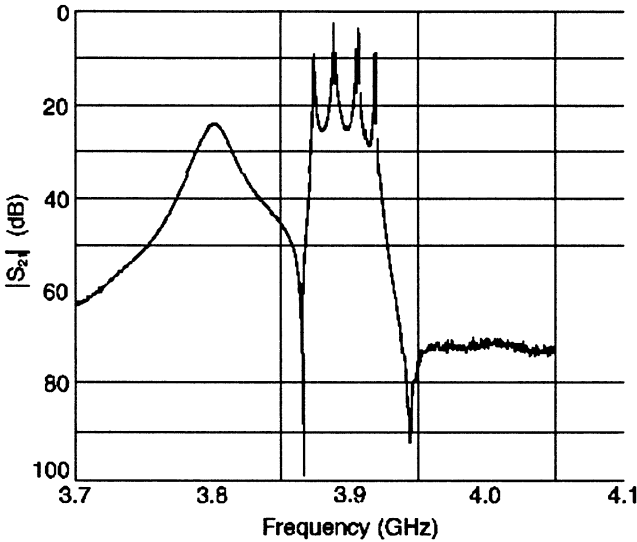
(b)

Bandler *et al.* "Electromagnetic design of HTS filters", **Figure 4**

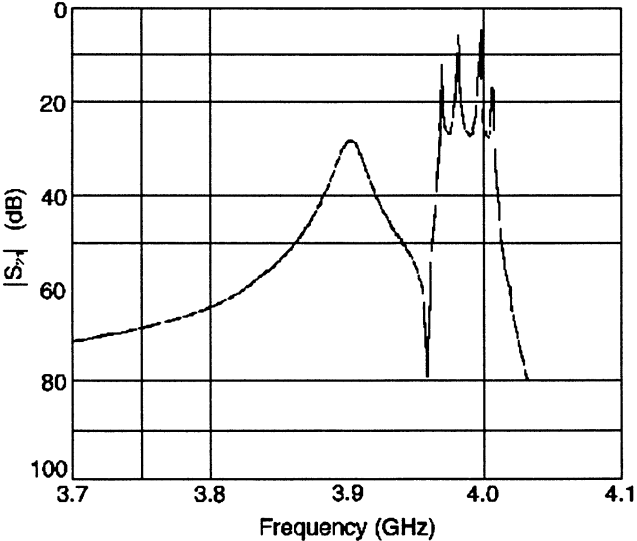
International Journal of Microwave and Millimeter-Wave Computer-Aided Engineering, vol. 5, 1995, Special Issue on Engineering Applications of Electromagnetic Field Solvers.



(a)



(b)



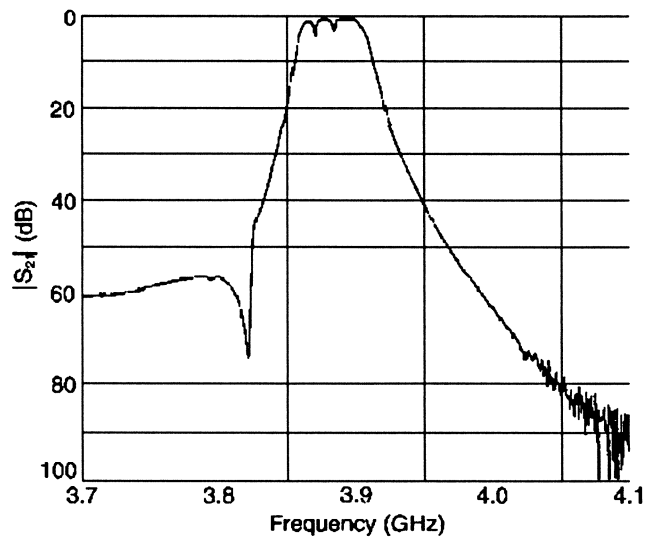
(c)

Bandler *et al.* "Electromagnetic design of HTS filters", **Figure 5**

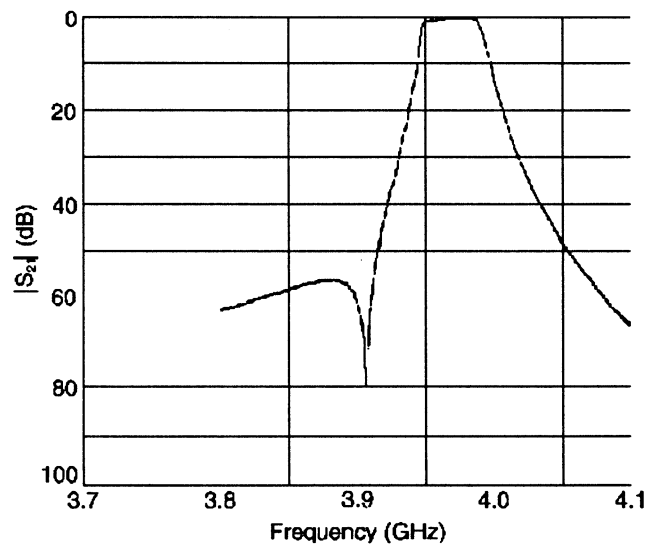
International Journal of Microwave and Millimeter-Wave Computer-Aided Engineering, vol. 5, 1995, Special Issue on Engineering Applications of Electromagnetic Field Solvers.



(a)



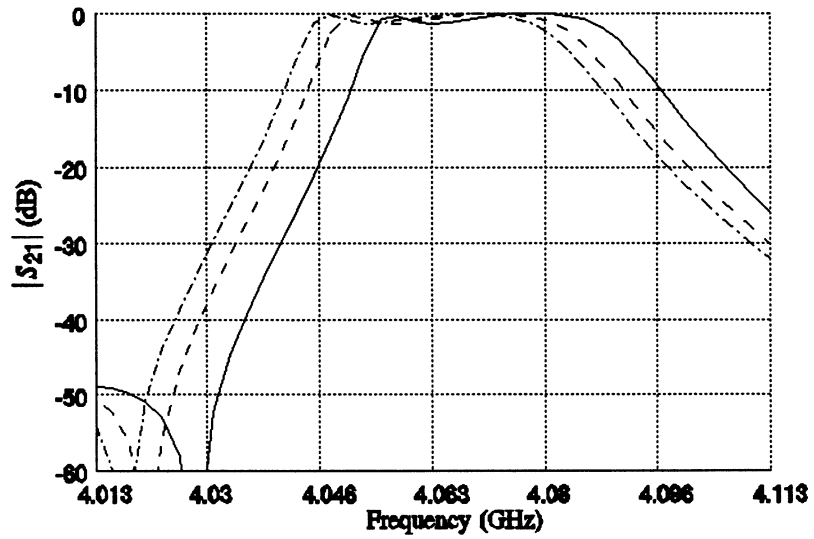
(b)



(c)

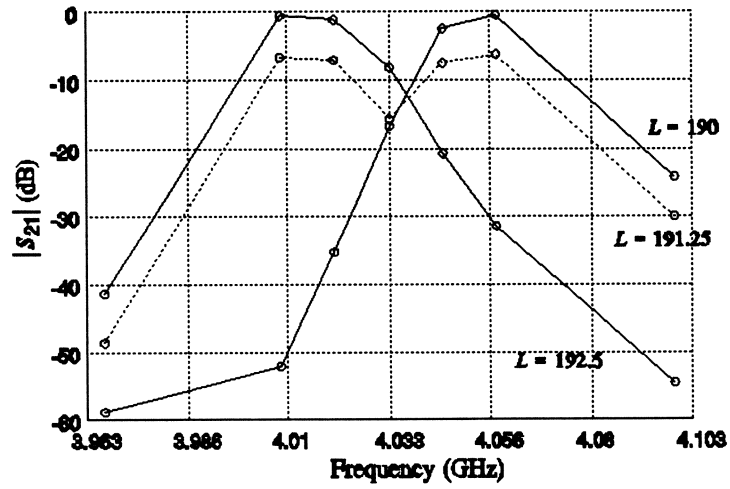
Bandler *et al.* "Electromagnetic design of HTS filters", **Figure 6**

International Journal of Microwave and Millimeter-Wave Computer-Aided Engineering, vol. 5, 1995,
Special Issue on Engineering Applications of Electromagnetic Field Solvers.



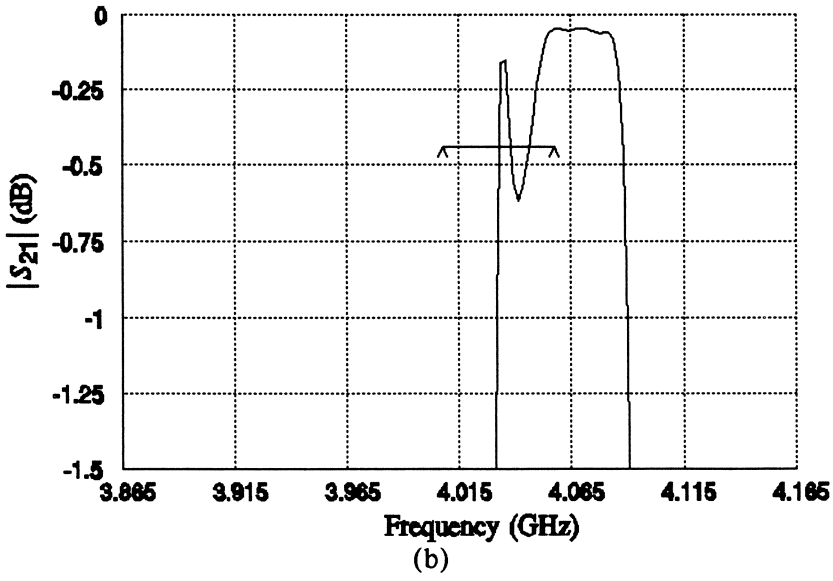
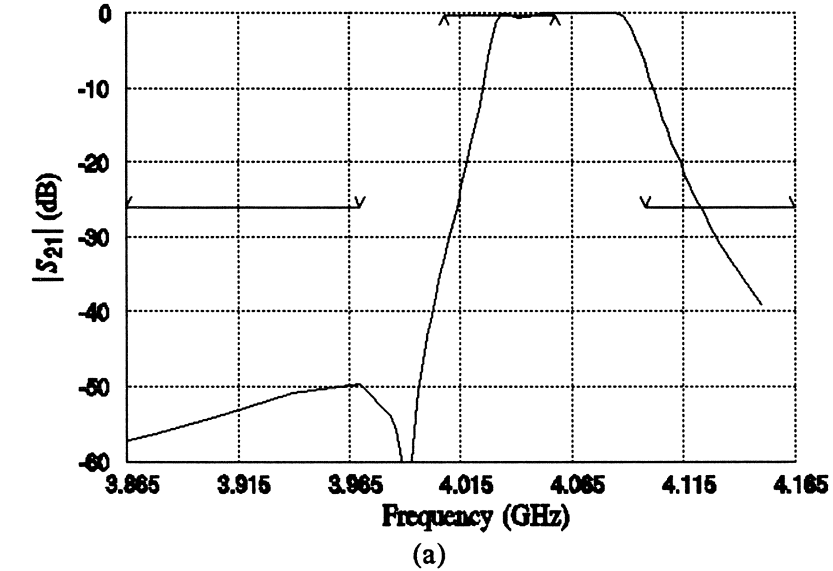
Bandler *et al.* "Electromagnetic design of HTS filters", **Figure 7**

International Journal of Microwave and Millimeter-Wave Computer-Aided Engineering, vol. 5, 1995,
Special Issue on Engineering Applications of Electromagnetic Field Solvers.



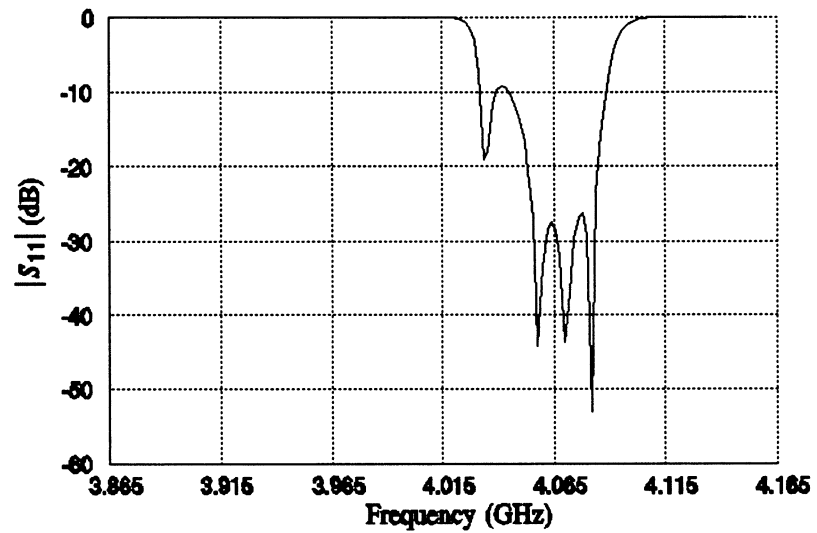
Bandler *et al.* "Electromagnetic design of HTS filters", **Figure 8**

International Journal of Microwave and Millimeter-Wave Computer-Aided Engineering, vol. 5, 1995, Special Issue on Engineering Applications of Electromagnetic Field Solvers.



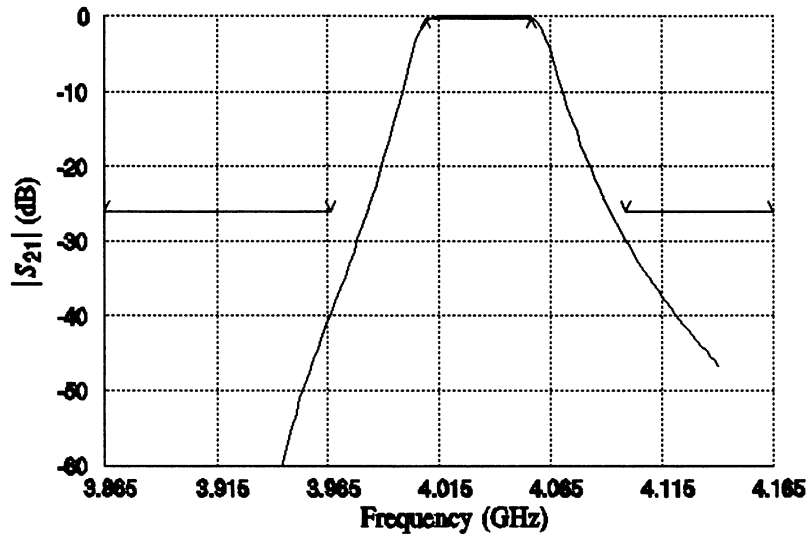
Bandler *et al.* "Electromagnetic design of HTS filters", **Figure 9**

International Journal of Microwave and Millimeter-Wave Computer-Aided Engineering, vol. 5, 1995,
Special Issue on Engineering Applications of Electromagnetic Field Solvers.

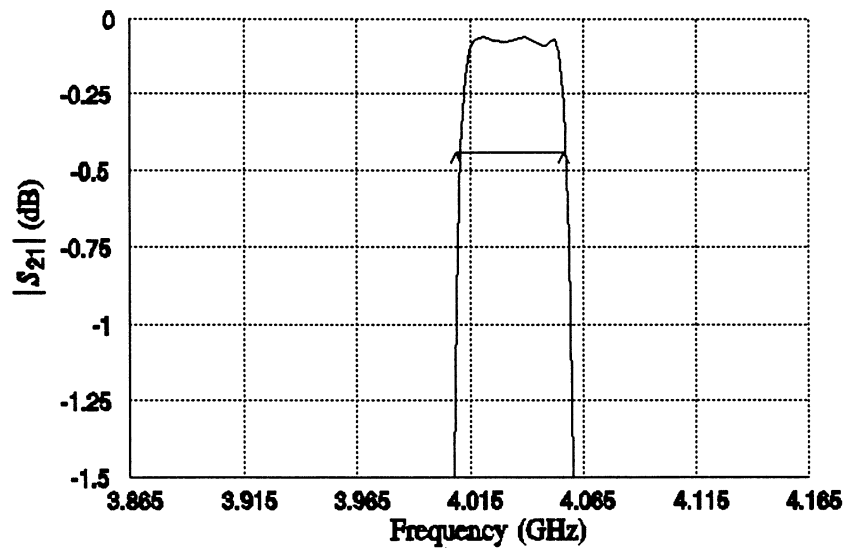


Bandler *et al.* "Electromagnetic design of HTS filters", **Figure 10**

International Journal of Microwave and Millimeter-Wave Computer-Aided Engineering, vol. 5, 1995, Special Issue on Engineering Applications of Electromagnetic Field Solvers.



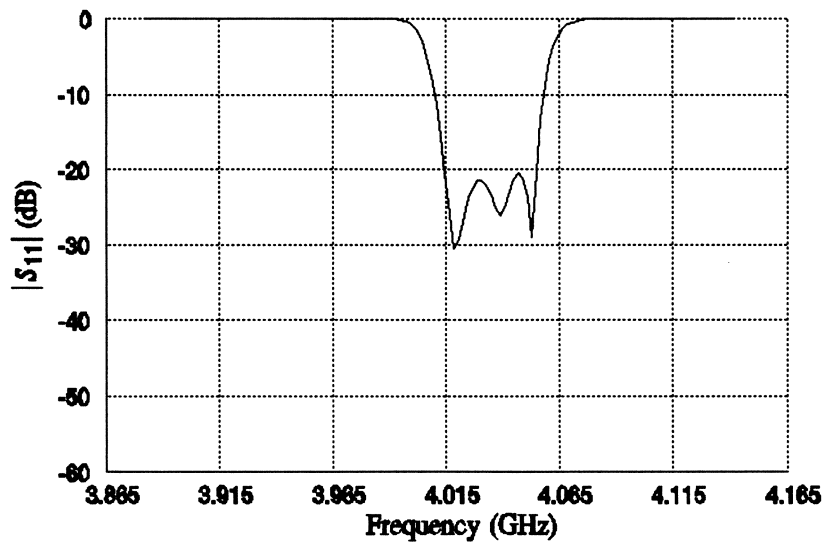
(a)



(b)

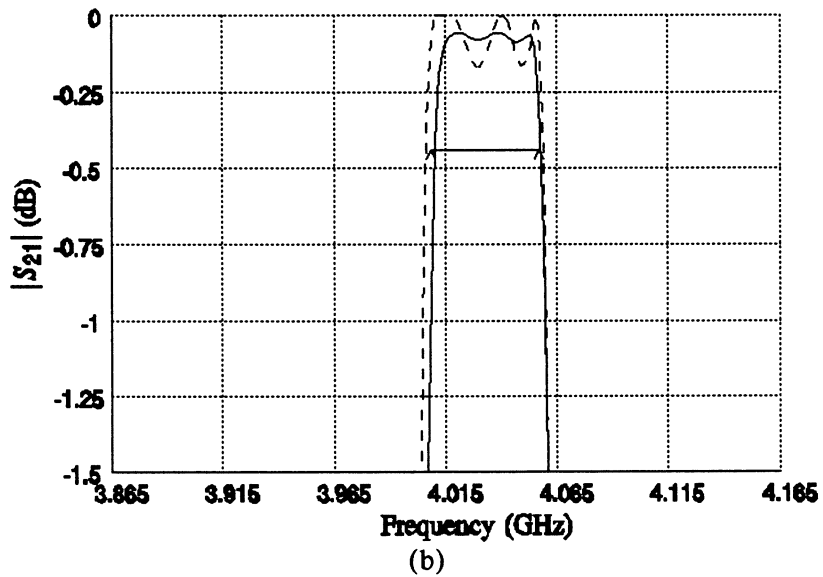
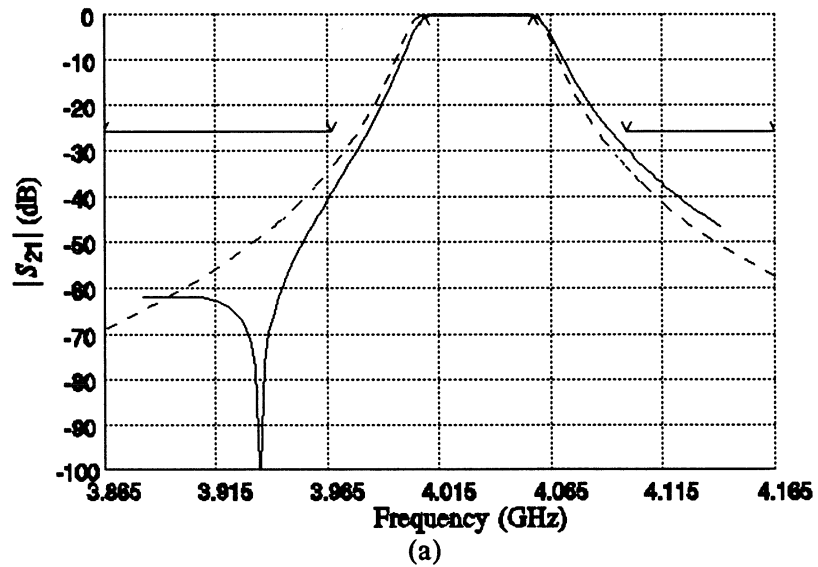
Bandler *et al.* "Electromagnetic design of HTS filters", **Figure 11**

International Journal of Microwave and Millimeter-Wave Computer-Aided Engineering, vol. 5, 1995,
Special Issue on Engineering Applications of Electromagnetic Field Solvers.



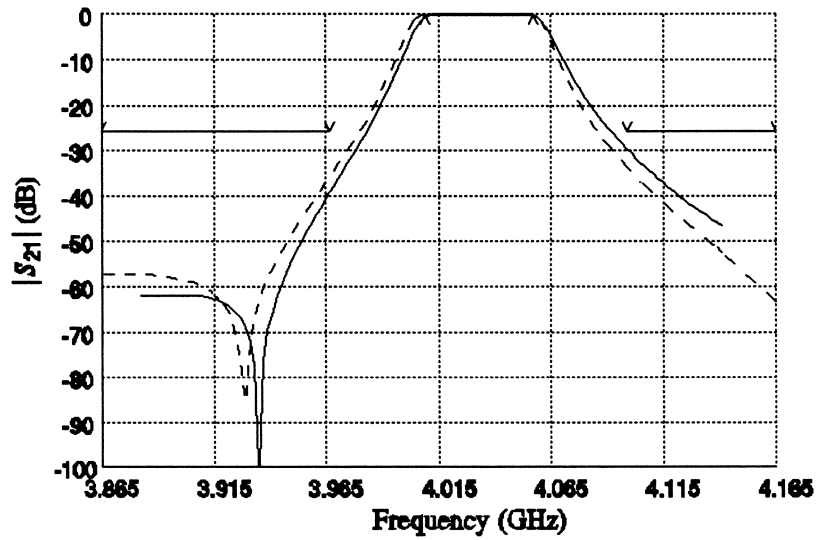
Bandler *et al.* "Electromagnetic design of HTS filters", **Figure 12**

International Journal of Microwave and Millimeter-Wave Computer-Aided Engineering, vol. 5, 1995,
Special Issue on Engineering Applications of Electromagnetic Field Solvers.

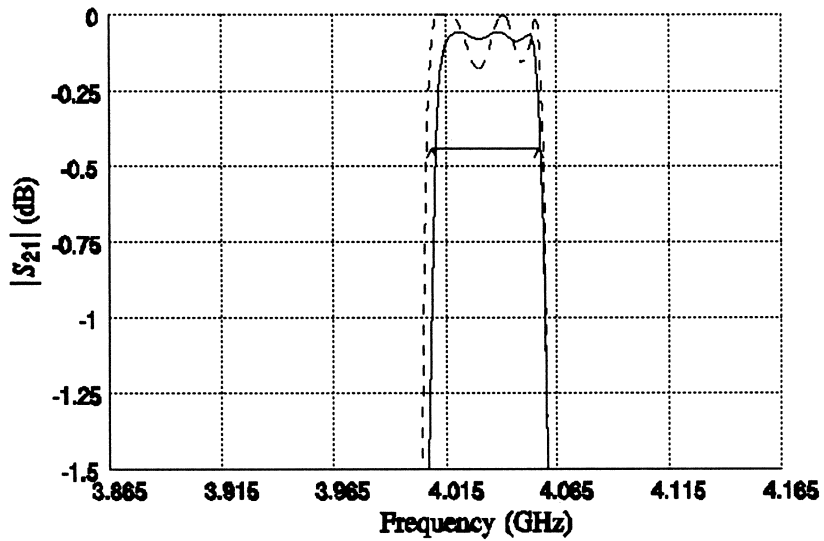


Bandler *et al.* "Electromagnetic design of HTS filters", **Figure 13**

International Journal of Microwave and Millimeter-Wave Computer-Aided Engineering, vol. 5, 1995, Special Issue on Engineering Applications of Electromagnetic Field Solvers.



(a)



(b)

Bandler *et al.* "Electromagnetic design of HTS filters",

***International Journal of Microwave and Millimeter-Wave Computer-Aided Engineering*, vol. 5, 1995,
Special Issue on Engineering Applications of Electromagnetic Field Solvers.**

